Chapter 9
Estimating Noise Spectra for Data from an Instrumented Building

Bryan S. Joyce and Pablo A. Tarazaga

Abstract Virginia Tech's Goodwin Hall is instrumented with over 200 highly sensitive, seismic accelerometers. These sensors detect motion from vibration sources inside the building (e.g. footsteps, HVAC equipment, and closing doors) and external (seismic motion and wind loading). The later sources produce much weaker excitations for the sensors and result in lower signal-to-noise ratios. Therefore, it is important to estimate the inherent noise present in the accelerometer signals in order to determine and analyze the actual building vibrations from seismic motion and wind loading. Sources of noise include electrical interference and self-noise in the instrumentation system including the accelerometers, cables, and signal conditioning amplifiers. This paper will examine several techniques for using collocated sensors for estimating the power spectral densities of the noise present in accelerometer measurements. First these estimation techniques are applied to simulated signals corrupted by noise. Then these methods are applied to laboratory data from several accelerometers placed on a vibration isolation table.

Keywords Noise estimation • Signal estimation • Signal-to-noise ratio • Collocated sensors • Common signal noise estimation

9.1 Introduction

Obtaining high quality data is an obvious priority in most experiments. Having a high signal-to-noise ratio (SNR) in all experimental measurements is important for reliable analysis [1, 2]. Here the signal from a sensor is defined as the portion of the measurement due to the physical input of interest. For accelerometers, the signal would be the portion of the output voltage due solely to the actual acceleration experienced by the proof mass. We define the term "noise" to mean any undesired contribution to the measurement, such as electrical interference in the transmission cables or self-noise from the sensor and data acquisition system [3]. Assuming the noise is additive to the signal, then the measurement $y(t)$ is the sum of the noise $n(t)$ and the signal $s(t)$, i.e.

$$y(t) = s(t) + n(t). \tag{9.1}$$

Ideally the noise amplitude should be small compared to that of the signal. However, this is not always possible, particularly in applications with small motions and thus small signals.

The Virginia Tech Smart Infrastructure Laboratory (VTSIL) has instrumented Goodwin Hall with over 200 high-sensitivity accelerometers. This highly instrumented building allows VTSIL to study the building's dynamics and activity of occupants among other topics. Work into localization and identification of people in the building has shown sufficiently large signals for analysis [4, 5]. As VTSIL begins analysis on building dynamics, obtaining good measurements from such weak oscillations becomes a concern. Seismic motion and wind loads on the building cause small excitations and thus small accelerations. While our accelerometers have a high sensitivity, it is still important to estimate the noise floor of these measurements. The noise floor needs to be estimated in terms of the overall noise power (for use in calculating a SNR) but also in terms of the power spectral density of the noise. It will be more difficult to estimate modal parameters in frequency bands with high noise power. Knowing the bands of high noise levels will aid later analysis. In addition, estimates of the noise spectra for the sensors can be used in simulations of building dynamics for studying data analyses techniques.

B.S. Joyce (✉) • P.A. Tarazaga
Department of Mechanical Engineering, Virginia Tech, Virginia Tech Smart Infrastructure Laboratory (VTSIL),
310 Goodwin Hall (MC 0238), 635 Prices Fork Road, Blacksburg, VA 24061, USA
e-mail: bsj@vt.edu

S. Atamturktur et al. (eds.), *Model Validation and Uncertainty Quantification, Volume 3*, Conference Proceedings
of the Society for Experimental Mechanics Series, DOI 10.1007/978-3-319-29754-5_9

There has been some work into estimating the noise levels in measured signals, particularly in the seismology community. These methods can broadly be organized into in situ and ex situ estimation techniques. For all of these methods, the accelerometer is connected to the same instrumentation equipment (cabling, signal conditioners, and data acquisition systems) that will be used in application. The ex situ noise estimation methods take the sensor out of operation. In some cases the accelerometer either in a "quiet" location with little excitation [6]. In this case, the signal is ideally close to zero and the measurement is assumed to be purely noise (see Eq. 9.1). However, this method is not feasible for high sensitivity accelerometers designed to detect the slightest ground motions. Other techniques will place the accelerometer on a shaker that applies a known excitation (often a sine wave) [7]. In this case, the uncorrupted signal $s(t)$ is known and the measured acceleration $y(t)$ is measured. Equation (9.1) leads to an estimation of the noise signal $n(t)$ or its power spectral density.

However, these methods often do not test the data acquisition system, cabling, and sensor *as installed for application*. Issues can be introduced in operation such as "misalignment noise" from improper sensor installation, electromagnetic interference in the sensors or cables, and acoustic effects [8]. Analysis of the sensor in situ provides a better estimate of the noise the sensor actually experiences in operation (because the estimation occurs while the sensor is in operation). If the accelerometer is also subject to normal operational conditions, then the in situ noise estimation techniques can also yield estimates of the signal spectrum.

The physical input to a seismic accelerometer (e.g. ground motion or wind motion) is often considered stochastic [1, 9]. Since the noise signal is often also stochastic, this makes separation of the signal from the noise more challenging. One solution to this problem is to use a set of collocated sensors. Several accelerometers in close proximity will experience nearly the same base motion. If the noise on each accelerometer is uncorrelated to each other or to the base motion (the signal), then the cross-correlation of the accelerometer measurements can lead to an estimate of the true, shared input signal, $s(t)$.

This paper will examine several noise estimation methods that use this multi-sensor approach. This paper will first present some terminology for use in later sections. Next some noise spectra estimation techniques are discussed. These are divided into two categories: methods that use two sensors and methods that use three sensors. These methods could be extended to included more than three sensors, but this is made more challenging in practice due to limits on the number of available sensors and available data acquisition channels. These methods are then applied to simulation data. Finally, these techniques are used to estimate noise spectra from sensors placed on a granite table.

9.2 Power Spectral Density (PSD) and Signal-to-Noise Ratio (SNR)

It is important to first define a few terms and state some necessary assumptions. Let the cross-correlation between the measurements from two accelerometers, $y_i(t)$ and $y_j(t)$, be denoted as $E[y_i(t)\ y_j(t+\tau)]$ where E is the expectation operator and τ is an arbitrary time delay. Then the cross-power spectral density (CPSD) is simply the Fourier transform of the cross-correlation, denoted as

$$G_{ij}(\omega) = G\left[y_i(t), y_j(t)\right] = F\left[E\left[y_i(t)\ y_j(t+\tau)\right]\right], \tag{9.2}$$

where F denotes the Fourier transform and $G[\bullet, \bullet]$ is defined here as the cross power spectral density operator [10, 11]. The result will be a function of frequency ω. The power spectral density (PSD) is calculated by applying the CPSD operator using the same signal for both operands, i.e.

$$G_{ii}(\omega) = G\left[y_i(t), y_i(t)\right] = F\left[E\left[y_i(t)\ y_i(t+\tau)\right]\right]. \tag{9.3}$$

In simulations and in experiments, the CPSDs and PSDs will be calculated using a pwelch method in MATLAB [12]. Note that because the accelerometer measurements are real-valued, only positive frequencies are considered, and one-sided PSDs will be used here.

The estimation methods in the next sections rely on a few assumptions. First assume we have collocated sensors measuring the same signal, $s(t)$. Also assume the signal and noise for each sensor (and consequently the measurement $y_i(t)$) have a zero mean value. This is justified as we will use IEPE accelerometers with AC coupling. Next assume the signal is uncorrelated to the noise. Also assume the noise on all of the sensors are uncorrelated to each other. Mathematically, these statements can be written as

$$E\left[s(t)n_i(t)\right] \quad and \quad E\left[n_i(t)n_j(t)\right] \quad for\ i \neq j \tag{9.4}$$

where $n_i(t)$ is the noise for accelerometer i. Note that no subscript is used for the signal as it is assumed the collocated accelerometers experience the same physical input and thus the same signal, $s(t)$. From this, the CPSD between the signal and noise on any channel is zero. Note that in practice the finite length of real signals will lead to a non-zero CPSD [13].

From Eq. (9.1) and the above assumptions, one can conclude that for any sensor i, the PSD of the measurement, $G_{ii}(\omega)$, can be written as

$$G_{ii}(\omega) = G_{ss}(\omega) + G_{n_i n_i}(\omega). \tag{9.5}$$

where $G_{ii}(\omega)$ is the PSD of the signal, $s(t)$ and $G_{n_i n_i}(\omega)$ is the PSD of the noise on sensor i, $n_i(t)$. If the PSD of the signal is known, then the noise PSD could be estimated easily from this equation. If the signal spectrum is known and the PSD of the measurement can be calculated from the measured data, then Eq. (9.5) will lead to an estimation of the noise spectrum. In application, the true signal is unknown and would also need to be extracted. In Sect. 9.5, "Estimator 1A" will use this method for comparison.

The power, or variance, of the signal is

$$\sigma_s^2 = \int_0^\infty (s(t))^2 \, dt = \int_0^\infty G_{ss}(\omega) \, df, \tag{9.6}$$

where the second equality comes from Parseval's theorem. A similar definition holds for the power of the noise $n_i(t)$ and the total measurement $y_i(t)$. Finally, we will take the signal-to-noise ratio for sensor i (SNR_i) as the variance of the signal divided by the variance of the noise, i.e.

$$SNR_i = \frac{\sigma_s^2}{\sigma_{n_i}^2} = \frac{\int_0^\infty (s(t))^2 \, dt}{\int_0^\infty (n_i(t))^2 \, dt} = \frac{\int_0^\infty G_{ss}(\omega) \, df}{\int_0^\infty G_{n_i n_i}(\omega) \, df}. \tag{9.7}$$

9.3 Two-Channel Estimation Methods

Several researchers have developed techniques for estimating the noise spectrum and the signal-to-noise ratio using two collocated accelerometers. This section discusses some of these methods. For all of them, it is assumed the accelerometers experience the same acceleration (common signal), but their noise spectra are independent and uncorrelated.

9.3.1 Estimator 2A: Holcomb 1989

Holmcomb is one of the first to develop a method for calculating instrument noise using collocated seismometers [2, 14, 15]. Because the noise contributions for the sensors are assumed to be independent of each other and the signal (Eq. 9.4), the cross power spectral density between measurements from the two sensors will simplify to be the signal spectrum, i.e.

$$G_{ss} = |G_{12}|, \tag{9.8}$$

where G_{12} is the cross power spectral density between measurements from two accelerometer, $y_1(t)$ and $y_2(t)$. The magnitude of the CPSD is used as this calculation may yield a complex-value while the true signal PSD is purely real. Note that the argument is dropped from the PSD for ease of notation. From this and Eq. (9.5), the noise PSD for sensor i is simply

$$G_{n_i n_i} = G_{ii} - |G_{12}| \quad for \;\; i = 1 \text{ or } 2. \tag{9.9}$$

9.3.2 Estimator 2B: Tasič 2012

Tasič and Runovc use a method which uses a reference accelerometer with a known noise spectra [8]. However, this method can be extended to a reference sensor with an unknown noise spectra by assuming both sensors have the same self-noise. In this case, the authors derive an expression for the mean noise PSD of the two sensors,

$$G_{nn} = \frac{G_{11} + G_{22}}{2} - |G_{12}|\,, \tag{9.10}$$

where G_{nn} is the average noise spectrum between the two sensors, G_{11} is the PSD of $y_1(t)$, G_{22} is the PSD of $y_2(t)$, and G_{12} is the CPSD between $y_1(t)$ and $y_2(t)$. The signal spectrum is assumed to be the same as Eq. (9.8).

9.3.3 Estimator 2C: Brincker 2007

Brincker and Larsen derive a similar common noise spectrum between two identical, collocated sensors as Tasič and Runovc [16]. However, their method uses a geometric mean in place of the arithmetic average of the two measurement PSDs, i.e.

$$G_{nn} = \sqrt{G_{11}G_{22}} - |G_{12}|\,, \tag{9.11}$$

where here G_{nn} is the geometric average of the noise spectrum between the two sensors. Equation (9.8) is used to estimate the signal PSD.

9.3.4 Estimator 2D: Rainieri 2014

Rainieri and Fabbrocino develop an alternative method for calculating the noise and signal spectra [9]. Expanding on their method, calculate the PSD of the difference between the two measurements, i.e.

$$G_{1-2,\ 1-2} = G\left[y_1(t) - y_2(t), y_1(t) - y_2(t)\right]. \tag{9.12}$$

From Eq. (9.1) and the assumptions of uncorrelated noise spectra, this reduces to

$$G_{1-2,\ 1-2} = G_{n_1n_1} + G_{n_2n_2}. \tag{9.13}$$

Note that the difference of the original measurement PSDs is

$$G_{11} - G_{22} = G_{n_1n_1} - G_{n_2n_2}. \tag{9.14}$$

Combining Eqs. (9.13) and (9.14) leads to estimates for the noise PSDs for each sensor,

$$G_{n_1n_1} = \frac{G_{1-2,\ 1-2} + (G_{11} - G_{22})}{2}, \tag{9.15}$$

$$G_{n_2n_2} = \frac{G_{1-2,\ 1-2} - (G_{11} - G_{22})}{2}. \tag{9.16}$$

Similarly, the PSD of the sum of the two accelerometer measurements is

$$G_{1+2,\ 1+2} = G\left[y_1(t) + y_2(t), y_1(t) + y_2(t)\right] = 4G_{ss} + G_{n_1n_1} + G_{n_2n_2}. \tag{9.17}$$

This leads to an estimate of the signal PSD as

$$G_{ss} = \frac{G_{1+2,\ 1+2} - (G_{n_1 n_1} + G_{n_2 n_2})}{4} = \frac{G_{1+2,\ 1+2} - G_{1-2,\ 1-2}}{4}. \tag{9.18}$$

9.4 Three-Channel Estimation Methods

Including a third, collocated sensor allows for redundancy and potentially improved accuracy. This section examines a few methods using three sensors.

9.4.1 Estimator 3A: Sleeman 2006

Sleeman et al. develop a noise spectra estimation method using three sensors [17]. Their method is similar to that of Holcomb (Estimator 2A). However, by using a third sensor, the authors can define a relative frequency response function (FRF) between any two of the sensors. Thus this method can compensate for any differences in the characteristics of the sensors.

In this method the improved estimate of the signal PSD is

$$G_{ss} = \left| h_{ij} G_{ij} \right|, \tag{9.19}$$

where h_{ij} is the relative frequency response function between sensors i and j using sensor k as a reference, i.e.

$$h_{ij} = \frac{G_{ik}}{G_{jk}}. \tag{9.20}$$

This is the same as the "H_3" formulation of the frequency response function from Ewins [10]. The noise spectra are estimated as

$$G_{n_i n_i} = G_{ii} - |G_{ss}| \ for \ i = 1,\ 2,\ 3. \tag{9.21}$$

9.4.2 Estimator 3B: Tasič 2012 Extended

In this work, we will also introduce an extension of the Tasič and Runovc method (Estimator 2B). We can compute averages of the PSD estimates from different pairs of the three sensors, i.e.

$$G_{ss} = \frac{|G_{12}| + |G_{13}| + |G_{23}|}{3}, \tag{9.22}$$

and

$$G_{nn} = \frac{G_{nn}^{12} + G_{nn}^{13} + G_{nn}^{23}}{3}, \tag{9.23}$$

where G_{nn}^{ij} is the noise PSD estimate from Estimator 2B using sensors i and j. Averaging the Estimator 2B results over all possible sensor pairings should yield more accurate signal and noise PSD estimates.

9.4.3 Estimator 3C: Brincker 2007 Extended

Similar to Estimator 3B, we introduce an extension to the Brincker and Larsen method (Estimator 2C) to include geometric averages of the original signal and noise estimations for two sensors, i.e.

$$G_{ss} = \left(|G_{12}|\,|G_{13}|\,|G_{23}|\right)^{1/3}, \tag{9.24}$$

and

$$G_{nn} = \left(G_{nn}^{12} G_{nn}^{13} G_{nn}^{23}\right)^{1/3}. \tag{9.25}$$

where here G_{nn}^{ij} is the noise PSD estimate from Estimator 2C using sensors i and j.

9.5 Simulation Results

These estimators are next tested on simulation data. Three types of common signals are examined: a sine wave, a low-pass filtered white noise input, and a white noise signal filtered by a dynamic system. The noise contributions to the measurements, $n_i(t)$, are constructed from filtered white noise. Each simulated channel has a different instance of noise, but the noise is derived from the same characteristics: white noise filtered by a second order, low pass Butterworth filter with a corner frequency of 200 Hz. The signal variance held constant at unity while the variance of the noise is altered for each condition.

For each simulation, the simulation time is 10 min and the sampling rate is 1000 Hz. The PSDs are calculated using MATLAB's pwelch function with a window size of 1/8th of the number of samples and an overlap of 7/8th of a window [12]. The 7/8th overlap was chosen based on analysis by Evans et al. to help smooth the spectra estimates [6]. The noise spectra are only computed for the first sensor. Finally, an additional estimator, Estimator 1A, is derived from Eq. (9.5) assuming the signal spectrum is known. While the signal spectrum will not be known in real world experiments, this method is useful for comparison to the other methods.

9.5.1 Sinusoidal Input

First a sine wave input is used with an amplitude of $\sqrt{2}$ (a variance of one) and a frequency of 100 Hz. Figure 9.1 shows the true and estimated PSDs for a case with a SNR of 20 dB. The PSD of the measured signal, G_{yy}, is composed of the sum of the noise and signal spectra. Estimator 3A and 2D show the most variation in the signal and noise PSDs while the other methods shows smoother calculations. Figure 9.2 plots the relative errors of the signal power estimation, the noise power estimation, and the signal-to-noise ratio. The relative errors are calculated as the estimated value over the true value. For all of the estimators, the error in the signal power estimation is low for high SNR (low noise power). This is intuitive as the measurement is dominated by the signal at high SNR, making estimation easier. For Estimators 1A and 2D show good prediction of noise power at low SNR. The error in noise estimation increases with SNR for Estimators 1A, 2A and 2D. For Estimators 2B, 2C, 3B, and 3C, the noise power estimation improves with increasing SNR, but these methods show larger errors at low SNR.

9.5.2 Filtered White Noise Input

Next a more broadband signal is used. The signal is constructed by filtering white noise by a third order Butterworth filter with a corner frequency of 100 Hz. Figures 9.3 and 9.4 show simulation results using the filtered white noise input case. The trends in the relative errors are similar to those seen for the sinusoidal input.

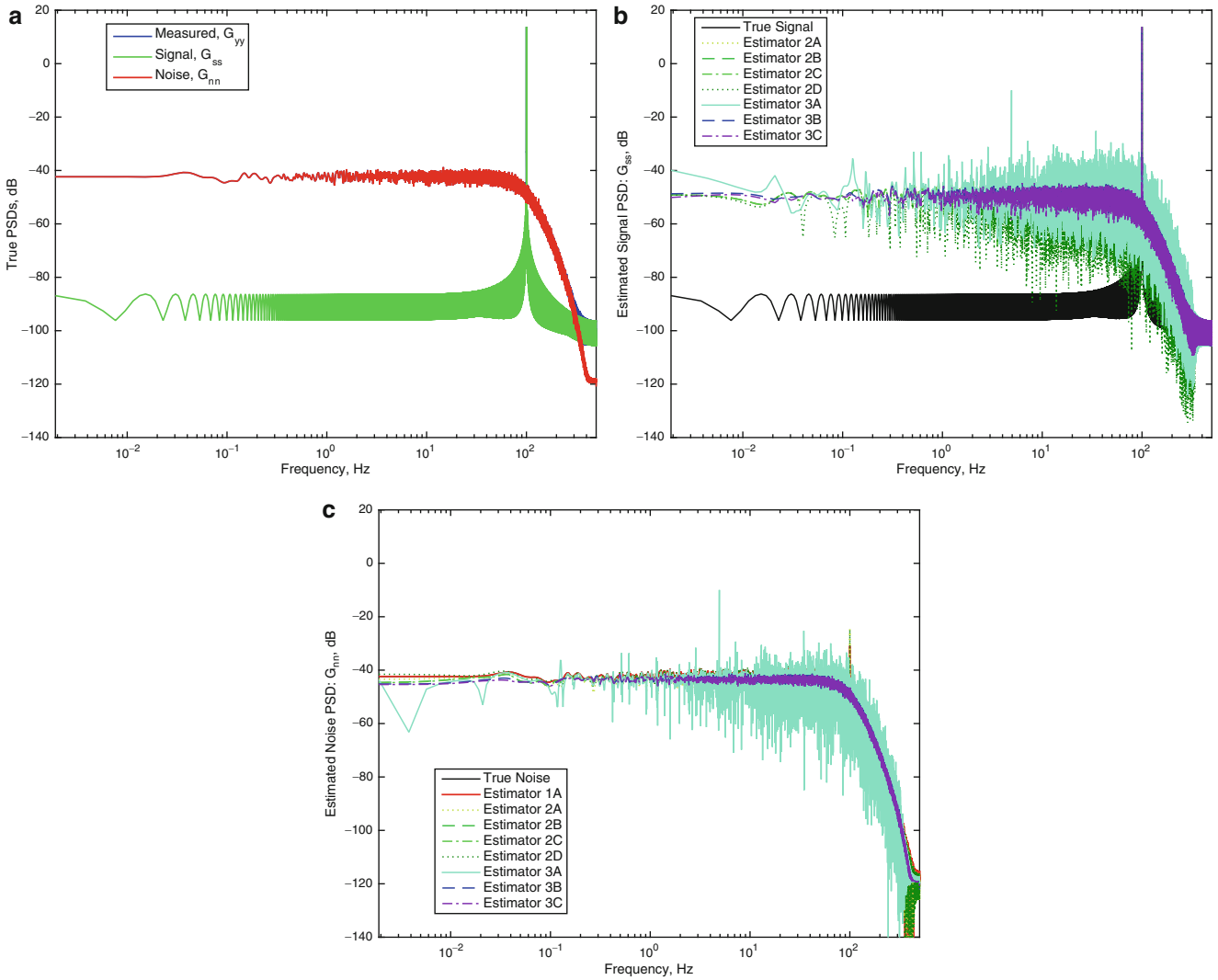

Fig. 9.1 PSDs and estimates for the measurement, signal, and noise with sine wave input at 100 Hz. Here the signal-to-noise ratio (SNR) is set to 20 dB. (**a**) The true PSDs, (**b**) estimated signal PSDs, and (**c**) estimated noise PSDs. In (**a**), the measurement PSD, G_{yy}, is behind the other PSDs

9.5.3 Dynamic Input

For the sensors in Goodwin Hall, a more realistic signal would be the acceleration of the building in response to a stochastic input. To simulated this, the low-pass filtered white noise signal used in Sect. 9.5.2 is used as input to a dynamic system. The output of this dynamic system is treated as the signal to the accelerometers, i.e. the signal $s(t)$ is constructed as

$$s(t) = \int_{\tau=0}^{t} h(t-\tau)\, w(\tau)\, d\tau, \tag{9.26}$$

where $w(t)$ is the filtered white noise from Sect. 9.5.2 and $h(t)$ is impulse response function of a dynamic system. The dynamic system is constructed using the Fourier transform of impulse response function, $H(\omega)$, in the form

$$H(\omega) = \sum_{i=1}^{5} \frac{A_i}{\omega_i^2 - \omega^2 + j2\zeta_i\omega\ \omega_i}, \tag{9.27}$$

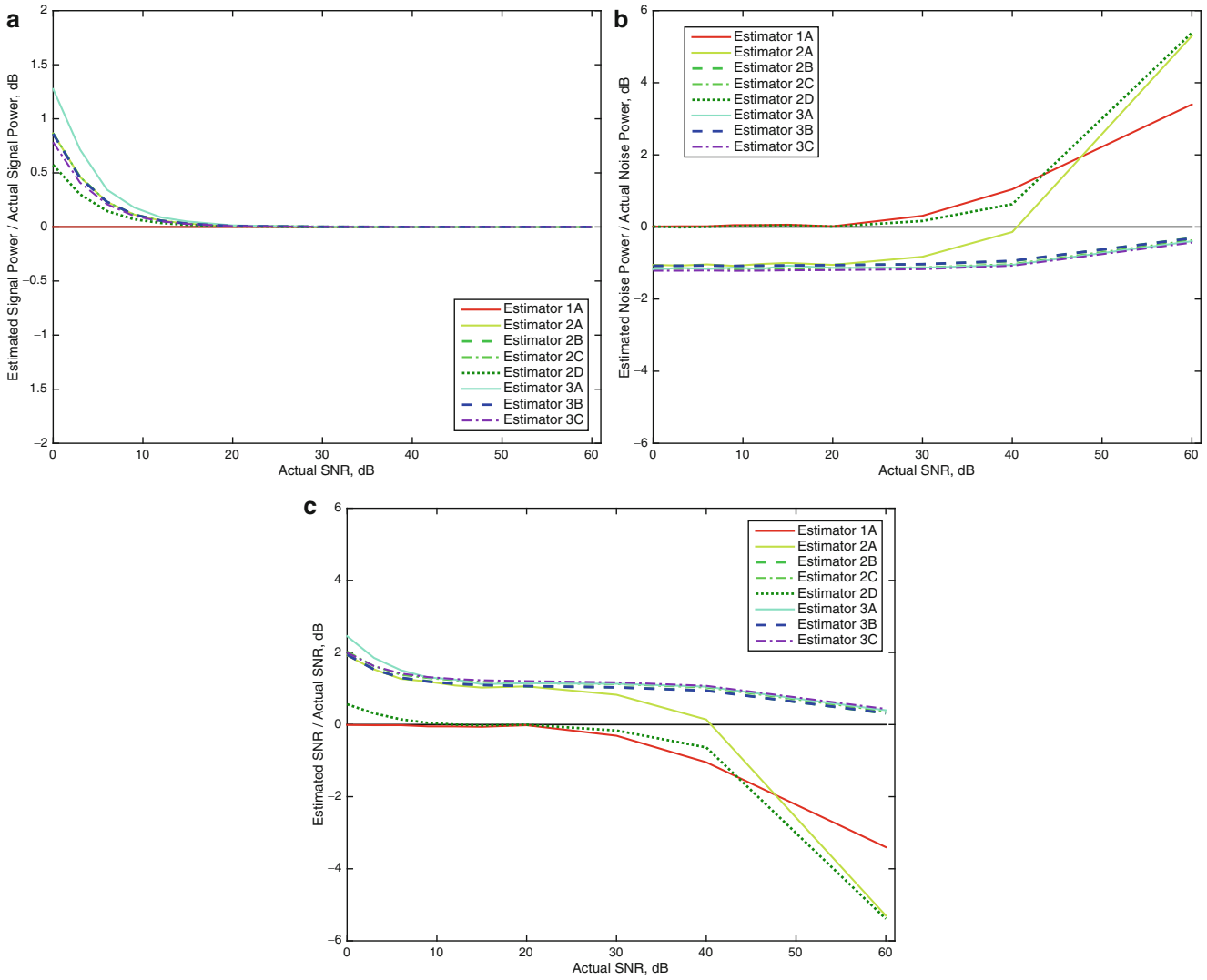

Fig. 9.2 Relative errors in (**a**) the signal power, (**b**) the noise power, and (**c**) the SNR estimations for a sinusoidal input

where ω_i is the natural frequency of mode i, ζ_i is the damping ratio, and A_i is the residue. Here five modes are used with natural frequencies of 0.1, 1, 3, 10, and 40 Hz. The damping ratios for all of the modes are 0.01. The residues (A_i) are 1 for first, third, and fourth modes and -1 for the second and fifth modes. Keeping the sign of the residue the same for the third and fourth modes produces an anti-resonance between the third and fourth modes. The final signal is then scaled to give a variance of one. Figures 9.5 and 9.6 show the simulation results for this case. The results show similar trends as the sine and random excitation case. Estimators 1A, 2A, and 2D show artificial increases in the noise power for frequencies where the signal power is large. This trend also appears for the sine wave input but is more evident here.

9.5.4 Summary of Simulation Results

For all of the inputs tested and for all of the estimation methods, the error in signal power is small for small noise levels. This follows from the measurement being dominated by the signal at low noise levels (making it more difficult to estimate the noise spectra). Estimators 3B and 3C show the smallest errors, and Estimators 2B and 2C also produce good results. This indicates that the averaging processes involved in these methods can improve the signal and noise estimations. Estimator 2D produces more accurate estimates of the overall noise power at low SNR, but produces noise and signal PSD estimates

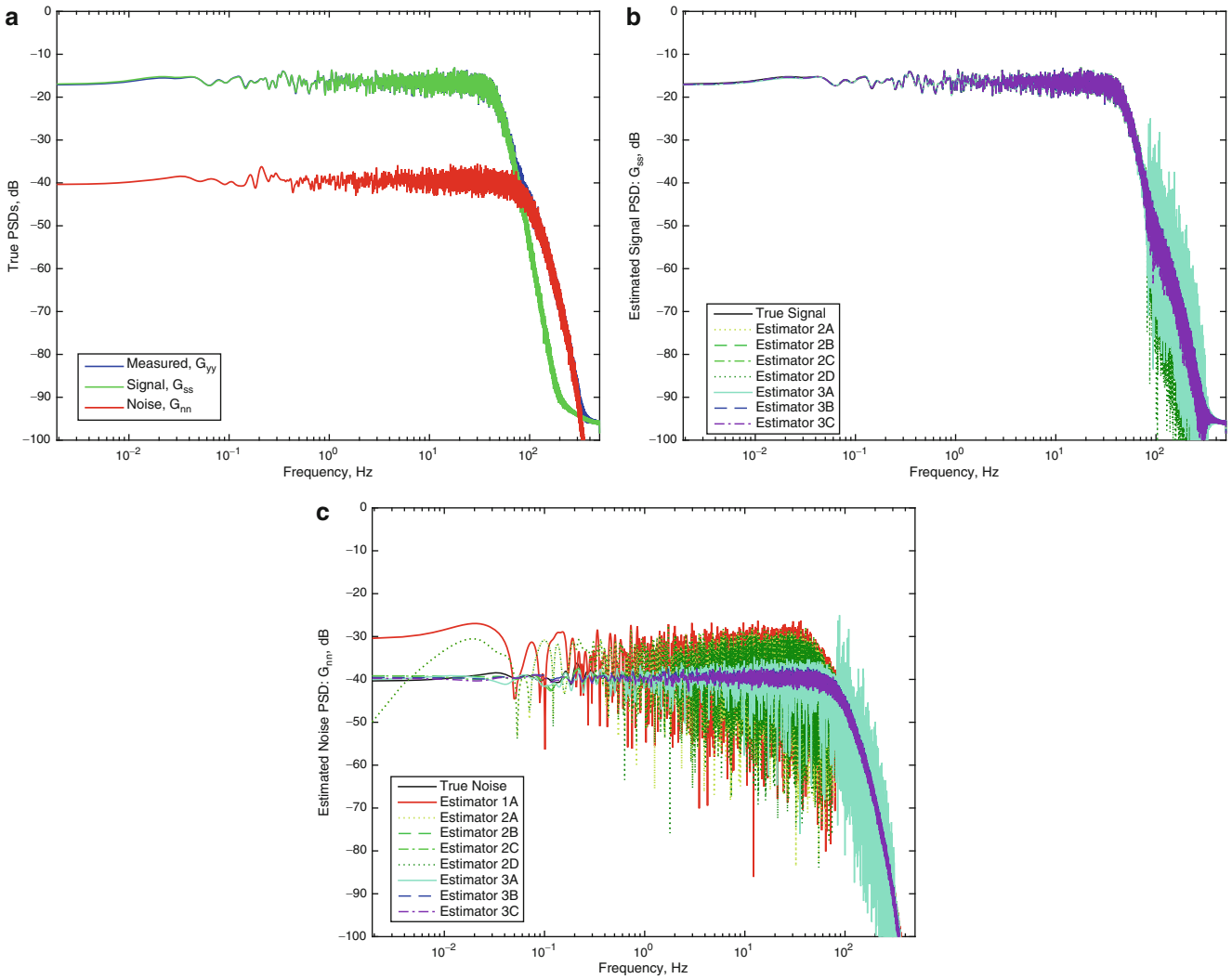

Fig. 9.3 PSDs and estimates for the measurement, signal, and noise with a filtered white noise input. The signal-to-noise ratio (SNR) is 20 dB. (**a**) The true PSDs, (**b**) estimated signal PSDs, and (**c**) estimated noise PSDs

with much larger variations than the other methods. Estimators 1A and 3A also show high variation with frequency in PSD estimations. Estimators 1A, 2A, and 2D produce noise power estimations which are too high for frequencies with high signal power.

9.6 Results from Lab Experiments

Next these noise estimators are applied to data from three collocated accelerometers on a granite table. Figure 9.7 shows the test setup. Four PCB 393B04 high sensitivity accelerometers are connected to small mounting pieces and then attached with wax to a granite table. Data is collected for all four sensors, but only three of the sensors will be used in this analysis. Each sensor is connected to a PCB 480C02 signal conditioner. Data is collected using a National Instruments NI 9215 with a 16 bit analog-to-digital convert (ADC). The voltage data from the accelerometers is scaled by each accelerometer's sensitivity (nominally 1000 mV/g). The channels are sampled at 1000 Hz for 10 min.

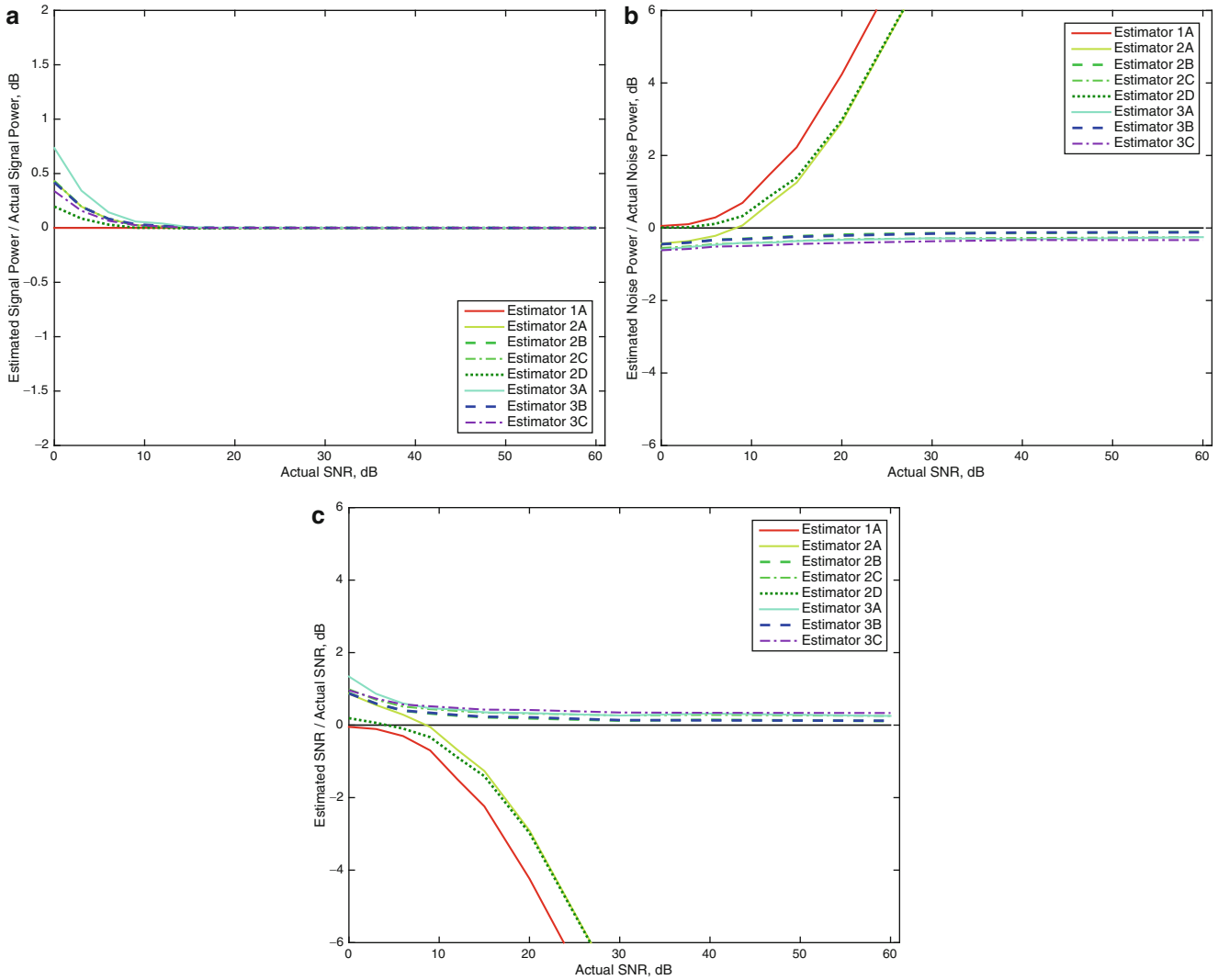

Fig. 9.4 Relative errors in (**a**) the signal power, (**b**) the noise power, and (**c**) the SNR estimations for a filtered white noise input

Figure 9.8a shows the time history of the acceleration signals, and Fig. 9.8b shows the computed power spectral densities. The PSDs show several large peaks. These peaks may be due to dynamics of the granite table or may be characteristic of the building's motion. For comparison, the plots also show the quantization noise expected from the analog-to-digital conversion. This forms a lower bound on the noise estimate. The power spectral density of the quantization noise (PSD_q) can be calculated as

$$PSD_q(\omega) = \frac{S^2\Delta^2}{24 f_s}, \tag{9.28}$$

where f_s is the sampling rate of the data acquisition system, Δ is the least significant bit (or quantization interval), and S is the sensitivity of the first accelerometer (used to compare the quantization PSD to that of the accelerometers) [17]. The sensitivity of the accelerometer is used to convert the quantization PSD from voltage to units of acceleration for ease of comparison. The quantization PSD for this accelerometer is about 1.7×10^{-11} g^2/Hz (-108 dB). In addition, the power spectral densities are also calculated with the data acquisition channel short-circuited and with the channel short-circuited after a 10 foot length of cable. These short circuit PSDs are shown in Fig. 9.8c. The short circuit noise is clearly above the quantization noise, however much of the PSD of the accelerometer signal is around the short-circuit PSD. Together, this analysis shows that much of the signal is dominated by the short circuit noise from the data acquisition system.

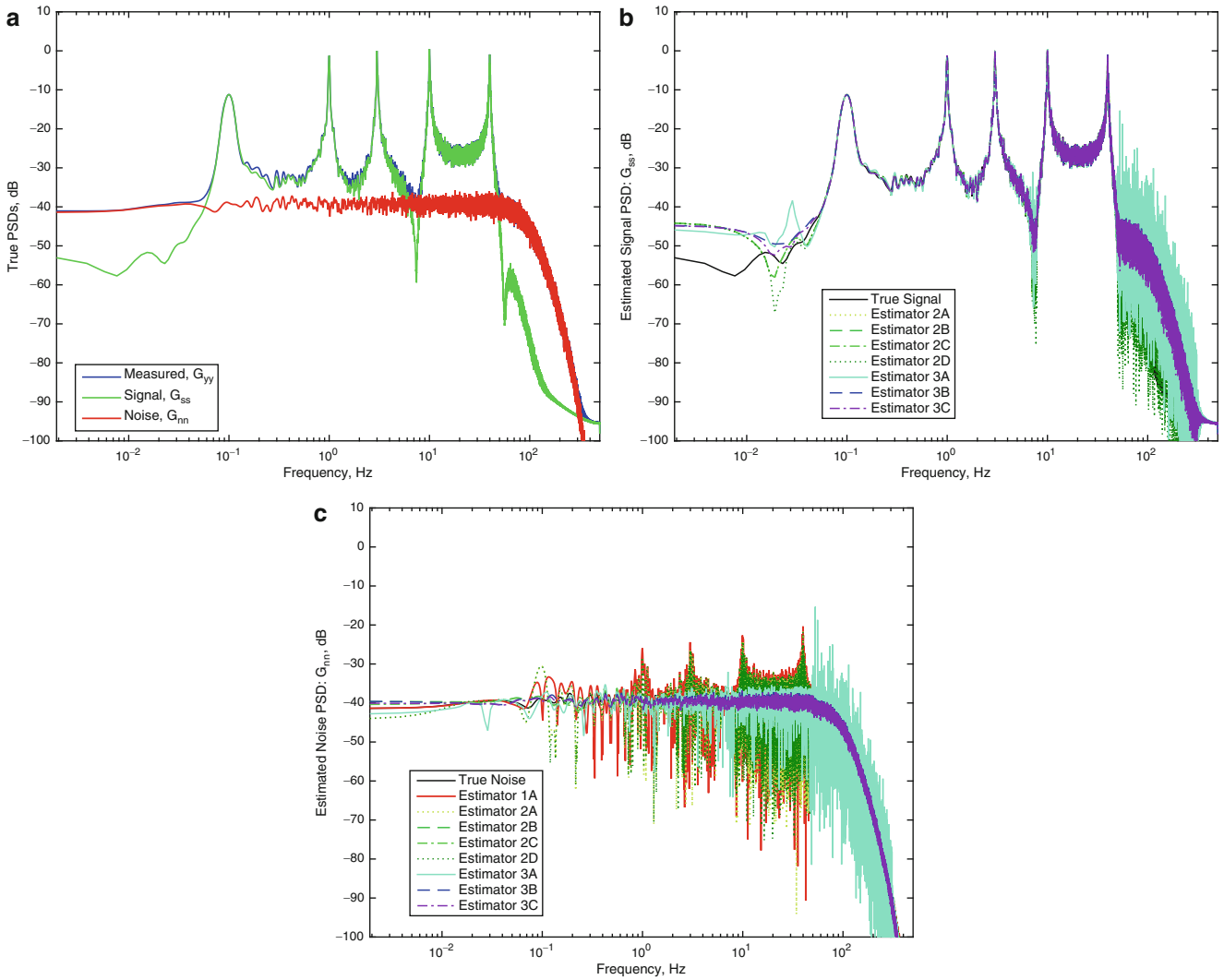

Fig. 9.5 PSDs and estimates for the measurement, signal, and noise with a dynamic input. The signal-to-noise ratio (SNR) is 20 dB. (**a**) The true PSDs, (**b**) estimated signal PSDs, and (**c**) estimated noise PSDs

Figure 9.9 plots the signal and noise PSD estimations. The noise PSDs are comparable to the short circuit PSD. The signal PSDs show features below the short circuit PSD (see between 1 and 5 Hz). Both of these show good promise that these methods are able to extract accurate signal and noise PSDs from real data. Table 9.1 summarizes the signal and noise powers from the different estimators. The powers and signal-to-noise ratios are calculated over a band from 0.1 Hz (the lowest frequency rating of the accelerometers) to the Nyquist frequency (500 Hz). The measurement power can also be calculated from the Estimators as the sum of the signal and noise power (second column in Table 9.1). For comparison, the variance of the first, second, and third accelerometer measurements is 2.36×10^{-7} g^2, 2.58×10^{-7} g^2, and 2.54×10^{-7} g^2, respectively, between 0.1 and 500 Hz. The variance in the short circuit condition was 1.14×10^{-7} g^2. Finally, the average SNR value over all of the estimators is 2.7 dB.

9.7 Conclusions and Future Work

This paper compares several methods for calculating the noise spectra in accelerometers using multiple, collocated sensors. Based on simulation and experimental data, the estimation methods using more accelerometers and using averaging techniques (Estimators 3B and 3C) yield the most accurate results at high to moderate signal-to-noise ratios. Experimental data for three accelerometers on a granite table shows low signal-to-noise ratio (around 2.7 dB).

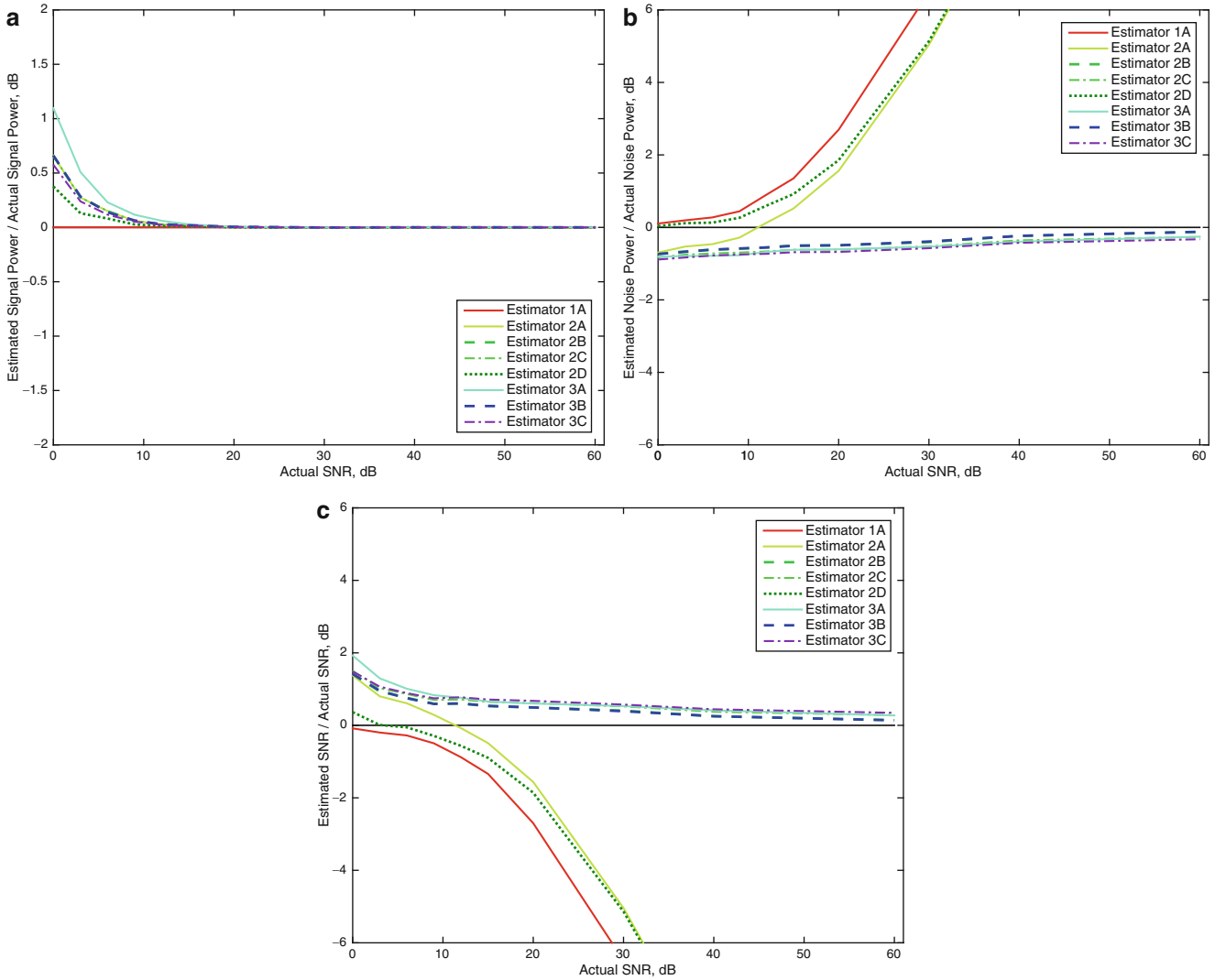

Fig. 9.6 Relative errors in (**a**) the signal power, (**b**) the noise power, and (**c**) the SNR estimations for a dynamic input

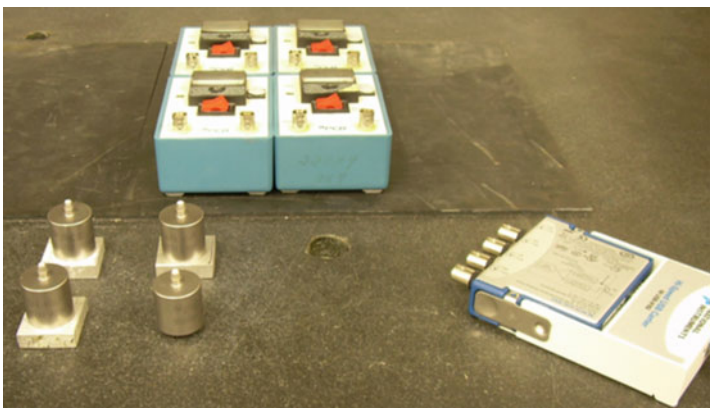

Fig. 9.7 Test setup for noise estimation. Data is recorded for four accelerometers, however data from the forth sensor is not used here

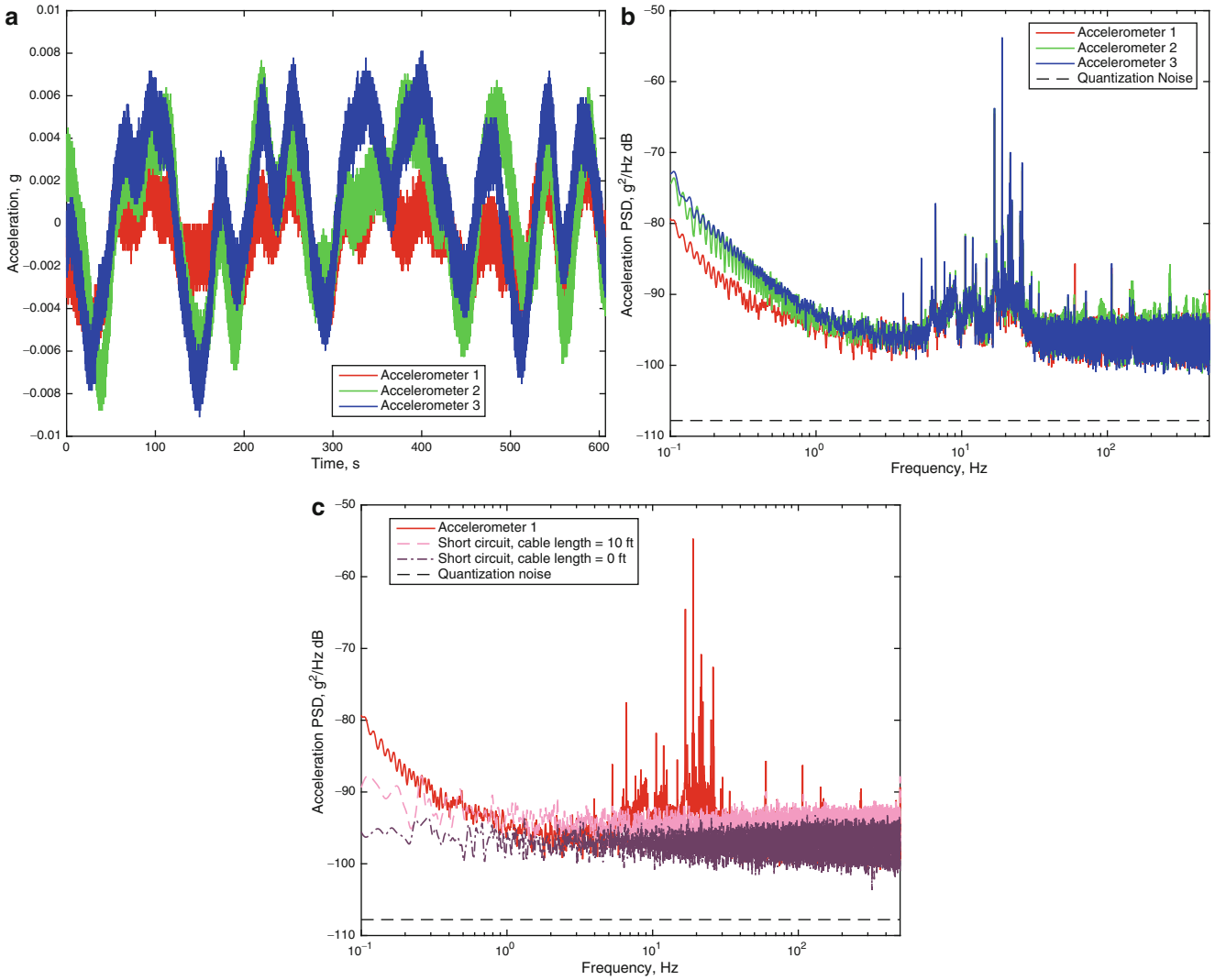

Fig. 9.8 (**a**) Time signals and (**b**) PSDs for the three accelerometers. (**c**) PSD of the first accelerometer compared to PSDs using a short circuit channel and a short circuit channel after a 10 foot cable

Future work will examine methods for improving these results as well as other algorithms for estimating the noise floor of a measurement. Using a different data acquisition system, oversampling, filtering, and altering parameters in the pwelch algorithm may improve these results. These techniques will also be applied to sample locations inside Goodwin Hall. The design of the mounts allows us to install multiple sensors in one location using an additional mounting piece. This data will lead to estimates of the acceleration in different locations, the noise spectra for different sensors with different cable lengths as installed in the building, and estimated signal-to-noise ratios for sensors throughout the instrumented building.

Acknowledgements The authors are thankful for the support and collaborative efforts provided by our sponsors VTI Instruments; PCB Piezotronics, Inc.; Dytran Instruments, Inc.; and Oregano Systems. The authors would also like to recognize the support from the College of Engineering at Virginia Tech, collaboration efforts with Gilbane, Inc., and financial support from the Student Engineering Council at Virginia Tech.

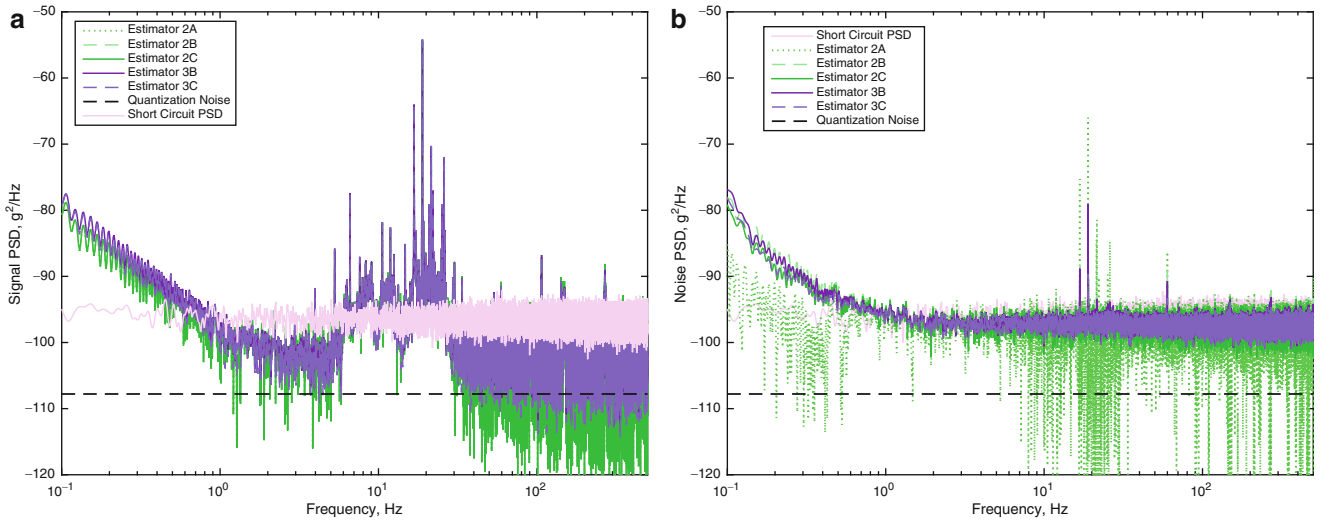

Fig. 9.9 Estimates of the (**a**) signal and (**b**) noise spectra for the first accelerometer signal. Estimators 2D and 3A show large variation and are omitted here for visual clarity

Table 9.1 Signal power, noise power, and signal-to-noise ratio (SNR) estimates for the lab experiment data

Estimator	Measurement power (g^2)	Signal power (g^2)	Noise power (g^2)	SNR (dB)
Estimator 2A	2.36×10^{-7}	1.62×10^{-7}	7.45×10^{-8}	3.4
Estimator 2B	2.58×10^{-7}	1.62×10^{-7}	9.61×10^{-8}	2.3
Estimator 2C	2.54×10^{-7}	1.62×10^{-7}	9.22×10^{-8}	2.4
Estimator 2D	2.37×10^{-7}	1.53×10^{-7}	8.37×10^{-8}	2.6
Estimator 3A	2.36×10^{-7}	1.64×10^{-7}	7.21×10^{-8}	3.6
Estimator 3B	2.58×10^{-7}	1.61×10^{-7}	9.65×10^{-8}	2.2
Estimator 3C	2.49×10^{-7}	1.58×10^{-7}	9.17×10^{-8}	2.4

Values are calculated from data between 0.1 Hz and the Nyquist frequency (500 Hz)

References

1. Brincker, R.: Some elements of operational modal analysis. Shock Vib. **2014**, 11 (2014)
2. Ringler, A.T., Hutt, C.R., Evans, J.R., Sandoval, L.D.: A comparison of seismic instrument noise coherence analysis techniques. Bull. Seismol. Soc. Am. **101**, 558–567 (2011)
3. Piersol, A.G.: Harris' Shock and Vibration Handbook, 6th edn. McGraw-Hill, New York (2010)
4. Poston, J.D., Schloemann, J., Buehrer, R.M., Sriram Malladi, V.V.N., Woolard, A.G., Tarazaga, P.A.: Towards indoor localization of pedestrians via smart building vibration sensing. In: 2015 International Conference on Localization and GNSS (ICL-GNSS), pp. 1–6 (2015)
5. Schloemann, J., Malladi, V.V.N.S., Woolard, A.G., Hamilton, J.M., Buehrer, R.M, Tarazaga, P.A.: Vibration event localization in an instrumented building. In: International Modal Analysis Conference (IMAC) XXXIII, Orlando, 2–5 February (2015)
6. Evans, J.R., Followill, F., Hutt, C.R., Kromer, R.P., Nigbor, R.L., Ringler, A.T., Steim, J.M., Wielandt, E.: Method for calculating self-noise spectra and operating ranges for seismographic inertial sensors and recorders. Seismol. Res. Lett. **81**, 640–646 (2010)
7. Payne, B.F., Serbyn, M.R.: An application of parameter estimation theory in low frequency accelerometer calibrations. Presented at the fourteenth transducer workshop, Colorado Springs, CO (1987)
8. Tasic, I., Runovc, F.: Seismometer self-noise estimation using a single reference instrument. J. Seismol. **16**(2), 183–194 (2012)
9. Rainieri, C., Fabbrocino, G.: Operational Modal Analysis of Civil Engineering Structures: An Introduction and Guide for Applications, 1st edn. Springer-Verlag, New York (2014)
10. Ewins, D.J.: Modal Testing: Theory, Practice, and Application, 2nd edn. Research Studies Press Ltd., Hertfordshire, England (2000)
11. Wirsching, P.H., Paez, T., Ortiz, K.: Random Vibrations: Theory and Practice. Wiley, New York (1995)
12. Welch, P.D.: The use of fast Fourier transform for the estimation of power spectra: a method based on time averaging over short, modified periodograms. IEEE Trans. Audio Electroacoust **15**(2), 70–73 (1967)
13. Steinhardt, A., Makhoul, J.: On the autocorrelation of finite-length sequences. IEEE Trans. Acoust. Speech Signal Process **33**(6), 1516–1520 (1985)
14. Holcomb, L.G.: A Direct Method for Calculating Instrument Noise Levels in Side-by-Side Seismometer Evaluations, pp. 89–214. U.S. Geological Survey, Albuquerque, New Mexico (1989)

15. Holcomb, L.G: A Numerical Study of Some Potential Sources of Error in Side-by-Side Seismometer Evaluations, pp. 90–406. U.S. Geological Survey, Albuquerque, New Mexico (1990)
16. Brincker, R., Larsen, J.A.: Obtaining and estimating low noise floors in vibration sensors. Presented at the 2007 IMAC-XXV: conference & exposition on structural dynamics (2007)
17. Sleeman, R., van Wettum, A., Trampert, J.: Three-channel correlation analysis: a new technique to measure instrumental noise of digitizers and seismic sensors. Bull. Seismol. Soc. Am. **96**(1), 258–271 (2006)